Chemical Geology 397 (2015) 14–23

Contents lists available at ScienceDirect

Chemical Geology

journal homepage: www.elsevier.com/locate/chemgeo

TIMS analysis of Sr and Nd isotopes in melt inclusions from Italian potassium-rich lavas using prototype 10^{13} Ω amplifiers

Janne M. Koornneef [a,*], Igor Nikogosian [a,b], Manfred J. van Bergen [b], Richard Smeets [a], Claudia Bouman [c], Gareth R. Davies [a]

[a] Faculty of Earth and Life Sciences, Vrije Universiteit Amsterdam, de Boelelaan 1085, 1081 HV Amsterdam, The Netherlands
[b] Department of Earth Sciences, Utrecht University, Budapestlaan 4, 3584 CD Utrecht, The Netherlands
[c] Thermo Fisher Scientific, Hanna-Kunath-Str. 11, 28199 Bremen, Germany

ARTICLE INFO

Article history:
Received 9 September 2014
Received in revised form 11 December 2014
Accepted 5 January 2015
Available online 20 January 2015

Editor: Catherine Chauvel

Keywords:
Melt inclusions
Sr Nd isotopes
TIMS
10^{13} Ω resistors
Potassium-rich lavas
Italy

ABSTRACT

Sr and Nd isotopes were determined using new thermal ionisation mass spectrometry (TIMS) techniques for a suite of 21 olivine-hosted (85–92 mol% Fo) melt inclusions selected from potassic and ultra-potassic lavas from the Italian peninsula. Sr isotopes were measured using default 10^{11} Ω resistors, whereas Nd isotope compositions were determined using new 10^{13} Ω resistors mounted in the amplifiers' feedback loop. Compared to default 10^{11} Ω resistors, use of 10^{13} Ω resistors results in a 10-fold improvement of the signal-to-noise ratio and more precise data when analysing small ion beams (<20 mV). A miniaturised Sr and Nd chemical separation procedure was developed to minimise total procedural blanks. Using the combined new chemical separation and TIMS analysis techniques samples as small as 2 ng Sr and 30 pg Nd were analysed successfully. $^{87}Sr/^{86}Sr$ ratios in the melt inclusions range from 0.70508 to 0.71543 and $^{143}Nd/^{144}Nd$ ratios range from 0.51175 to 0.51268. Significant differences in $^{87}Sr/^{86}Sr$ and $^{143}Nd/^{144}Nd$ were found between melt inclusions and host lavas indicating distinct evolution paths for the lava groundmasses and the primitive melts that were trapped in the olivine phenocrysts. In line with magmatic processes known to have affected Italian potassic volcanics, the observed differences between inclusions and host lavas can be attributed to (1) mixing and mingling of isotopically distinct magma batches, (2) assimilation of crustal material with different isotope compositions, and (3) early (incomplete) mixing of primitive melts derived from an isotopically heterogeneous mantle source. These data demonstrate the potential of the analysis of Sr and Nd isotope ratios in individual melt inclusions for detailed studies of magma mixing and evolution processes.

1. Introduction

Advances in the detection system of mass spectrometers allow increasingly smaller geological samples to be precisely analysed for their isotope composition (Tuttas et al., 2007, 2008; Jakopič et al., 2009; Wielandt and Bizzarro, 2011; Koornneef et al., 2013; Liu and Pearson, 2014). An important new development has been the fabrication of 10^{13} Ω resistors mounted in the feedback loop of Faraday cup amplifiers (Koornneef et al., 2014). Use of these 10^{13} Ω resistors in the detection of ion beams results in a 100 times higher output V compared to default 10^{11} Ω amplifiers. At the same time the electrical noise level only increases by a factor of 10, resulting in a 10-fold improvement of the signal-to-noise ratio. The 10^{13} Ω amplifiers therefore produce more precise data on small ion beams compared to the conventional 10^{11} Ω amplifiers used in Faraday detection. Prototype 10^{13} Ω amplifiers were recently tested in thermal ionisation mass spectrometry (TIMS) analyses of Sr and Nd isotope compositions in reference materials, demonstrating their excellent performance (Koornneef et al., 2014).

In this manuscript we present a first application of the use of amplifiers equipped with the new 10^{13} Ω resistors; determination of the Sr and Nd isotope compositions of individual melt inclusions by TIMS. Melt inclusions are trapped by crystals growing from melts accumulating in a magmatic system. With respect to bulk rock lavas, melt inclusions have been shown to record more extreme isotopic heterogeneity suggesting that melt extraction from the mantle may involve the accumulation of multiple melts derived from different sources (Saal et al., 1998, 2005; Jackson and Hart, 2006; Maclennan, 2008; Sobolev et al., 2011). Analyses of radiogenic isotopes in individual melt inclusions are challenging because of their size and the resulting amount of material available for analysis. To date Sr and Pb isotope data have been obtained by application of in situ analytical techniques, either secondary ion mass spectrometry (SIMS) or laser ablation (multi-collector) inductively coupled plasma mass spectrometry (LA-ICPMS). Here we report the first Sr and Nd isotope data on individual melt inclusions obtained using combined wet chemistry techniques and

* Corresponding author.
E-mail address: j.m.koornneef@vu.nl (J.M. Koornneef).

http://dx.doi.org/10.1016/j.chemgeo.2015.01.005
0009-2541/

TIMS analysis. The advantage over in situ techniques is that our measurements do not suffer from potential isotope fractionation associated with matrix effects and interfering elements (e.g. ^{87}Rb) as we use chemical separation to eliminate elements other than Sr and Nd.

Olivine-hosted melt inclusions from seven volcanic centres along the Italian peninsula were analysed. The subduction related potassic and ultra-potassic lavas from the Italian peninsula are especially suitable for this application as they are rich in incompatible elements and display a large range in Sr–Nd–Pb isotope compositions (Civetta et al., 1991; Conticelli and Peccerillo, 1992; Conticelli et al., 2002, 2011; Peccerillo, 2005; Peccerillo and Lustrino, 2005). The isotopic heterogeneity recorded in lavas from the region has been attributed to variable mantle source contamination by subducted continental components (Foley, 1992; Conticelli et al., 2002; Avanzinelli et al., 2009). Furthermore, there is widespread evidence for mixing/mingling between different magma series and shallow-level crustal contamination (Vannucci et al., 2006; Nikogosian et al., 2007; Nikogosian and van Bergen, 2010; Rose-Koga et al., 2012; Schiavi et al., 2012).

The specific aims of this study were to: (1) demonstrate that we can precisely and accurately determine the $^{87}Sr/^{86}Sr$ and $^{143}Nd/^{144}Nd$ isotope ratios of individual melt inclusions using the prototype 10^{13} Ω resistors and (2) explore the extent to which isotopic compositions of melt inclusions can differ from bulk host lavas placing more quantitative constraints on the evolution of the magmatic system.

2. Sample selection

For this study we selected twenty-one olivine hosted melt inclusions from eleven lavas collected from seven volcanic centres along the Italian peninsula (Fig. 1). Host lavas belong to lamproitic (LMP), silica-undersaturated leucite-bearing high-potassic (HKS), shoshonitic (SHO), high potassium calcalkaline (HKCA) and calc alkaline (CA) rock series (Table 1). The lavas are all younger than 0.8 Ma and cover a large and representative range of Sr and Nd isotope compositions. The host olivines of the selected melt inclusions have high forsterite contents (85–92 mol% Fo) to ensure the (near) primary nature of the trapped melts. Such primitive melt inclusions are a promising target as they might be isotopically distinct from bulk lavas if magmas were affected by mingling between different series and/or assimilation. Moreover, primitive inclusions potentially preserve pre-entrapment isotopic heterogeneity of melts extracted from a heterogeneous mantle source.

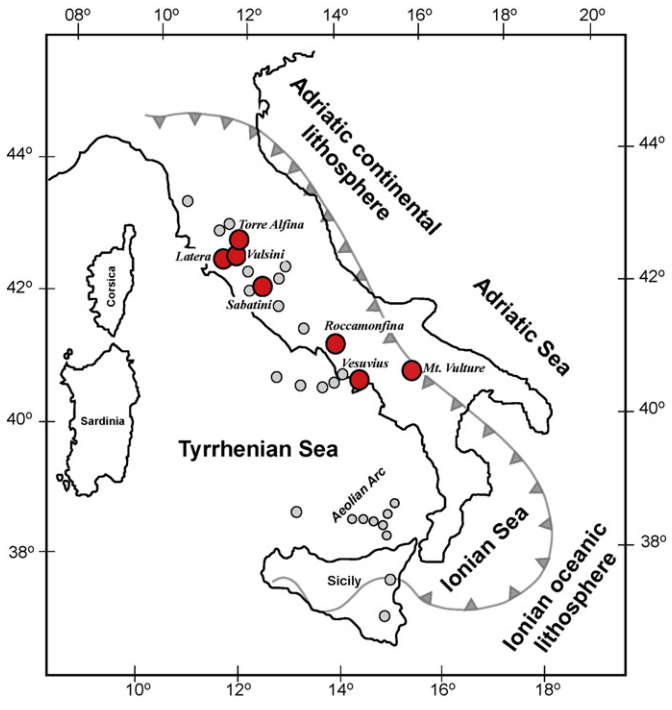

Fig. 1. Map of the Italian peninsula region showing the locations for samples used in this study (red circles) as well as other Pliocene–Quaternary Italian volcanic centres (grey circles). Map modified by Peccerillo (2005).

A key sample selection criterion was the required inclusion size to obtain accurate Sr and Nd isotope data (Fig. 2). All olivine hosted melt inclusions were previously homogenised and analysed by electron microprobe and secondary ionisation mass spectrometry (Nikogosian et al., 2007; Nikogosian and van Bergen, 2009, 2010) and thus had known major and trace element concentrations. Compared to host lavas the melt inclusions show significant major and trace element variability. Fig. 3 presents the Sr and Nd concentrations for inclusion and host lavas for the Roccamonfina locality as an example. The equivalence between the average composition of a set of melt inclusions and their host lava indicates that a whole-rock sample represents a mixture of heterogeneous melts that are preserved in early crystallised olivine. Melt inclusions with variable trace-element concentrations were selected, so that relationships between trace element and isotope compositions could be investigated. We selected host olivine with single melt inclusions using an optical microscope. Based on known Sr and Nd concentrations and approximate volume of an inclusion, the available amount of Sr and Nd could be estimated. Fig. 2 shows the relation between melt inclusion diameter and the concentration required for the minimum amount of material needed for a precise and accurate analysis: 2 ng Sr and 30 pg Nd (see Section 3.3). Sizes and concentrations for the selected melt inclusions are listed in Table 1. At least two melt inclusions were analysed from each locality. Images of representative samples are shown in Fig. 4.

3. Materials and methods

3.1. Miniaturised chemical separation of Sr and Nd

For isotopic analysis of the melt inclusion a miniaturised chemical procedure was developed to separate Sr and Nd and minimise the handling steps and amounts of acids and resins and hence keep procedural blank levels to a minimum.

Host olivines with the selected individual melt inclusions were removed from the epoxy mounts and dissolved together with the melt inclusions. Laser ablation ICPMS data established that Sr and Nd contents in olivine were near and below detection levels; at least lower than 0.1 ppm for Sr and 0.02 ppm for Nd (see also De Hoog et al., 2010). We thus assume that the olivine does not contribute significantly to the Sr and Nd isotope budgets of the melt inclusions. Before dissolution the olivine grains were cleaned with ultrapure acetone to remove potential contamination from sample preparation and handling. Samples were dissolved in Teflon vials in a 9:1 mix of HF and HNO_3 on a hotplate at 120 °C for 3 days. Sr and rare earth elements (REEs) were separated from the matrix in a setup whereby Sr Resin columns (Eichrom Technologies 50 μl resin, 100–150 μm mesh) were placed directly above TRU Resin columns (Eichrom Technologies, 150 μl resin, 100–150 μm mesh; Fig. 5). The Sr Resin columns were made of 1 ml pipette tips (PE, Greiner Bio-one) using a 3.5 mm PE frit (Angst and Pfister, h = 2 mm, porosity 35 μm). TRU resin columns were made of disposable Pasteur pipettes (PE, diameter of 3.4 mm) cut to obtain a height of 17 mm using a frit with 3.5 mm diameter. By placing the Sr column above the TRU Resin column during loading and washing, the pre-fraction from the Sr Resin column (in 3 M HNO_3) was directly eluted onto the TRU Resin column, after which the two column sets were separated and Sr and REE were eluted (Fig. 5 see also Mikova and Denkova, 2007). The Nd was further purified from the REE fraction in a Ln Resin column procedure modified after Pin and Zalduegui (1997). The columns were made of disposable Pasteur pipettes (PE, diameter of 3.4 mm) cut to obtain a height of 80 mm with a Ln resin

Table 1
Selected melt inclusions.

Volcanic centre	Age (ka)	Host lava	Sample	Fo olivine	MI type	Size (μm)[a]	Sr (ppm)	Sr (ng)[b]	Nd (ppm)	Nd (ng)[b]
Torre Alfina	800	LMP	TA-15	90.2	LMP	150	1295	9	320	2
		LMP	TA-66	88.5	LMP	150	1318	9	133	0.9
Vulsini	210	HKS	Vul-28	91.6	HKS	150	775	5	53	0.4
		HKS	Vul-21	91.8	HKS	200	925	12	64	0.8
Sabatini	206	HKS	Sab-224	90.2	HKS	150	1710	12	90	0.6
		HKS	Sab-85	90.9	HKS	160	1660	12	88	0.6
Latera	157	SHO	Lat-222	89.1	SHO-I	150	470	3	33	0.2
		SHO	Lat-220	89.1	SHO-I	220	543	7	34	0.4
		SHO	Lat-256	89.3	SHO-II	150	350	2.2	55	0.4
		SHO	Lat-157	89.1	SHO-II	100	203	0.3	16	0.03
Roccamonfina	150–500	HKS	Rocc7-8	87.0	HKS	70	2306	1.3	111	0.06
		HKS	Rocc7-265/9	87.4	HKS	100	2295	2.7	110	0.13
		SHO	Rocc5-40	89.3	HKS	220	1225	7	61	0.4
		HKCA	Rocc6-107	90.7	CA	250	813	17	28	0.6
		HKCA	Rocc6-104	90.7	SHO	150	1030	7	36.8	0.26
Vesuvius	1.8	HKS	Ves2B-187	87.9	HKS	120	870	2	66	0.12
		HKS	Ves2B-176/9	88.1	HKS	140	862	6	62	0.4
		HKS	Ves2L-152	89.0	HKS	150	722	5	42	0.3
Vulture	629	HKS	Melf7-57	85.3	HKS	250	896	20	102	2.5
		HKS	Melf7-82	88.6	HKS	150	2000	14	50	0.35
		HKS	Melf7-244	89.3	HKS	200	4583	55	143	1.8

[a] Size represents the estimated diameter of the melt inclusion determined by optical study.
[b] The amount of Nd and Sr is calculated based on the inclusion's optically estimated volume.

volume of 0.74 ml (Eichrom Technologies, 50–100 mm mesh). See Fig. 5 for the detailed elution schemes. Total procedural blanks varied between 3 and 20 pg for Sr and were below 2 pg for Nd. The blanks were determined by isotope dilution using an ^{84}Sr spike and a ^{150}Nd spike respectively. The host lavas were processed using standard Sr and Nd separation procedures (Koornneef et al., 2009; Font et al., 2012).

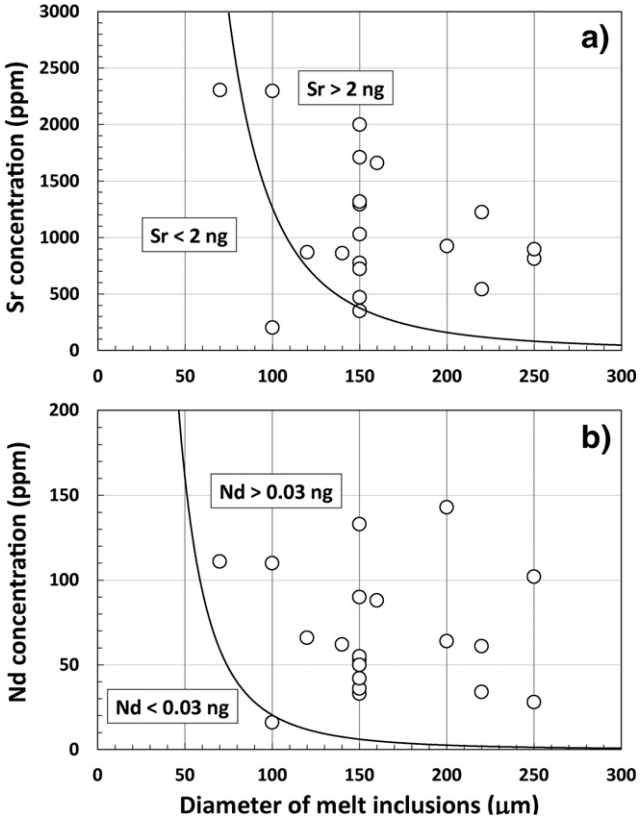

Fig. 2. Relationships between required melt inclusion size (diameter in μm) and element concentration for Sr (a) and Nd (b), based on the minimum amount (2 ng of Sr and 30 pg of Nd) needed for a reliable analysis of $^{87}Sr/^{86}Sr$ and $^{143}Nd/^{144}Nd$. Calculations assume a spherical melt inclusion geometry. Inclusions that fall on the right of the minimum curves qualify for analysis with the presented techniques. Symbols represent selected melt inclusions analysed in this study.

3.2. Mass spectrometry

Sr and Nd analyses were performed on a Thermo Scientific Triton-*Plus* TIMS at the VU University, Amsterdam. Sr/Nd ratios in most mantle derived rocks are above 20. Hence we were able to perform Sr isotope analyses using default 10^{11} Ω amplifiers in the feedback loop of the Faraday detectors whereas Nd analyses were undertaken using 10^{13} Ω amplifiers. For a detailed description of the 10^{13} Ω resistor analysis techniques the reader is referred to Koornneef et al. (2014) and only a brief summary is given here.

Four prototype 10^{13} Ω (recently released and available as a product) and six default 10^{11} Ω amplifiers were installed in a Triton *Plus*. Each of the amplifiers can be connected to any Faraday cup through the virtual amplifier relay matrix (Schwieters and H. Lerche, Thermo Electron (Bremen), US Patent 6,472,659 B1, issued 29/10/2002). For Nd analyses 10^{13} Ω amplifiers were connected to L2, L1, C, and H1 to measure masses ^{143}Nd to ^{146}Nd. An 11 minute baseline was measured during heating of the sample and subtracted online from the raw intensity values. Instrumental mass fractionation was corrected for using the exponential law and a $^{146}Nd/^{144}Nd$ value of 0.7219. The La Jolla reference standard was

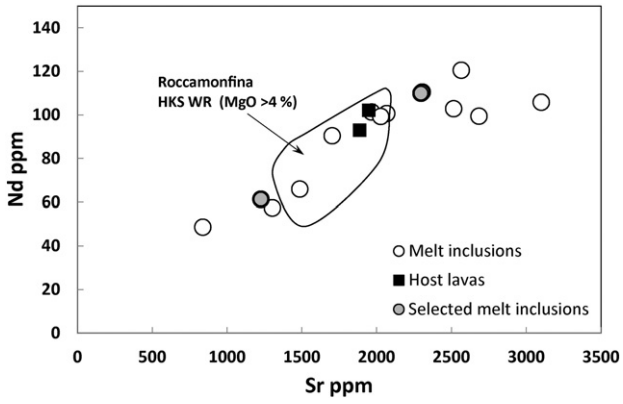

Fig. 3. Sr and Nd variability of melt inclusions from Roccamonfina compared to whole-rock compositions. Note that the whole-rock compositions are close to the averages of the melt inclusions, indicating that a lava sample is a mixing product of melts similar to those included in its olivines. Melt inclusions selected for this study are indicated.
Data are from Nikogosian and van Bergen, 2010.

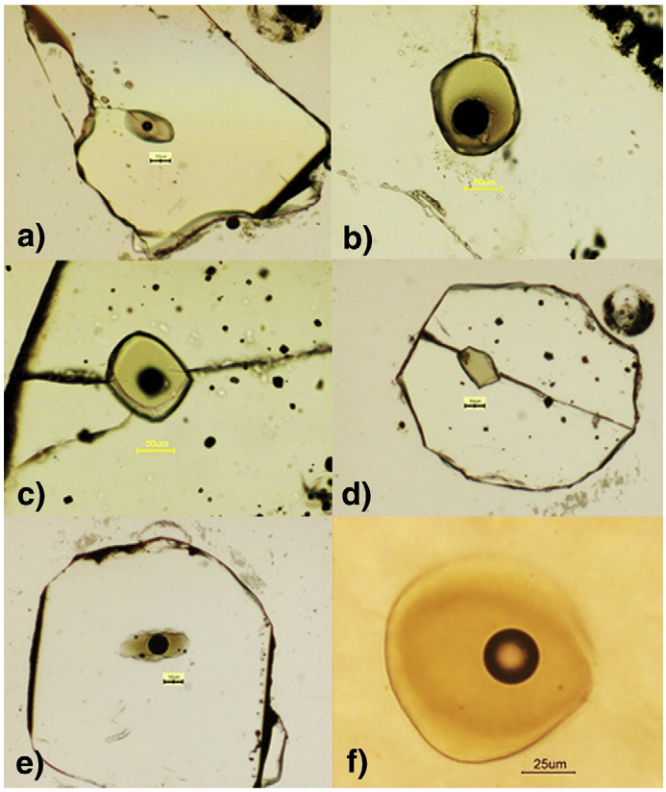

Fig. 4. Microphotographs of melt inclusions within their host olivine that were analysed for Sr and Nd isotope compositions. Inclusions from (a) Vulsini, (b) Latera, (c) Sabatini, (d) Roccamonfina, (e) Vulture, and (f) Vesuvius are shown as examples. Note that cracks are secondary and formed mechanically during preparation and handling. Spinel inclusions as observed in olivine grains from Sabatini and Roccamonfina do not influence the Sr and Nd isotope analyses as they contain negligible amount of Sr and Nd.

analysed once a day to perform an external gain correction on the mass bias corrected $^{143}Nd/^{144}Nd$ using the reference value of 0.511841 ± 0.000002 (Jochum et al., 2011). The 2SE error on this analysis was propagated into the final error on the $^{143}Nd/^{144}Nd$ and typically represented 10% of the total error. The gains for the 10^{13} Ω amplifiers were set to 1 in the software (executive table). Beam intensities were always kept below 3 V (30 mV if measured on a 10^{11} Ω amplifier). Samples were loaded on out-gassed annealed Re filaments with 1 μl H_3PO_4 and run to exhaustion to obtain the best in-run precision. A minimum of 60 cycles (8 s integration each) was collected, but on average samples ran for 168 cycles. For two of the larger samples the analyses on the 10^{13} were stopped after ≥260 cycles and re-analysed using 10^{11} Ω amplifiers as a secondary check on the accuracy (Section 3.4; Table. 2). Small, 100 pg, aliquots of our in house Nd standard (CIGO) were measured next to our samples to check for accuracy and reproducibility ($^{143}Nd/^{144}Nd$ = 0.511322 ± 104, n = 7). Accuracy is confirmed by the excellent agreement with the long-term average of CIGO determined on default 10^{11} Ω amplifiers: $^{143}Nd/^{144}Nd$ = 0.511333 ± 11, n = 72. Host lavas were measured using default 10^{11} Ω amplifiers.

3.3. Validation by rock standard analyses

International rock standards AGV-1 and BHVO-2 were used as secondary standards to validate our combined miniaturised chemical separation method and analytical procedures. Initial tests explored the minimum amount of material that could be processed and analysed. Aliquots of AGV-1 containing 50, 100, 150, 200 and 500 pg Nd were loaded onto the columns. The corresponding amounts of Sr were 1, 2, 3, 4 and 10 ng. The obtained data are shown in Fig. 6 Although all the Nd data are both accurate and reproducible, the Sr data become less accurate for smaller sample aliquots. The off-set of the measured $^{87}Sr/^{86}Sr$ towards higher values for aliquots lower than 2 ng can be explained by a contribution from a procedural chemistry blank. We determined the isotope composition of our total procedural chemical blank through a test in which we multiplied all used materials by a factor of 30 and obtained $^{87}Sr/^{86}Sr$ = 0.71112 ± 5, n = 3. Using this value, the observed off-set for samples below 2 ng can be explained by a total procedural blank of 7–10 pg. Measurements of samples smaller than 2 ng Sr thus preferably require a blank correction, necessitating the amount of Sr in the sample to be known accurately. Nd analyses do not suffer from procedural blanks, samples as small as 30 pg can be analysed precisely. Interspersed with our samples we processed four aliquots of AGV-1 and four aliquots of BHVO-2 containing ~3 ng Sr and 150–200 pg Nd. AGV-1 gave $^{143}Nd/^{144}Nd$ = 0.512759 ± 75 and $^{87}Sr/^{86}Sr$ = 0.704009 ± 10, 2SD n = 4 in excellent agreement with its reference values 0.512790 ± 20 and 0.703999 ± 60, respectively

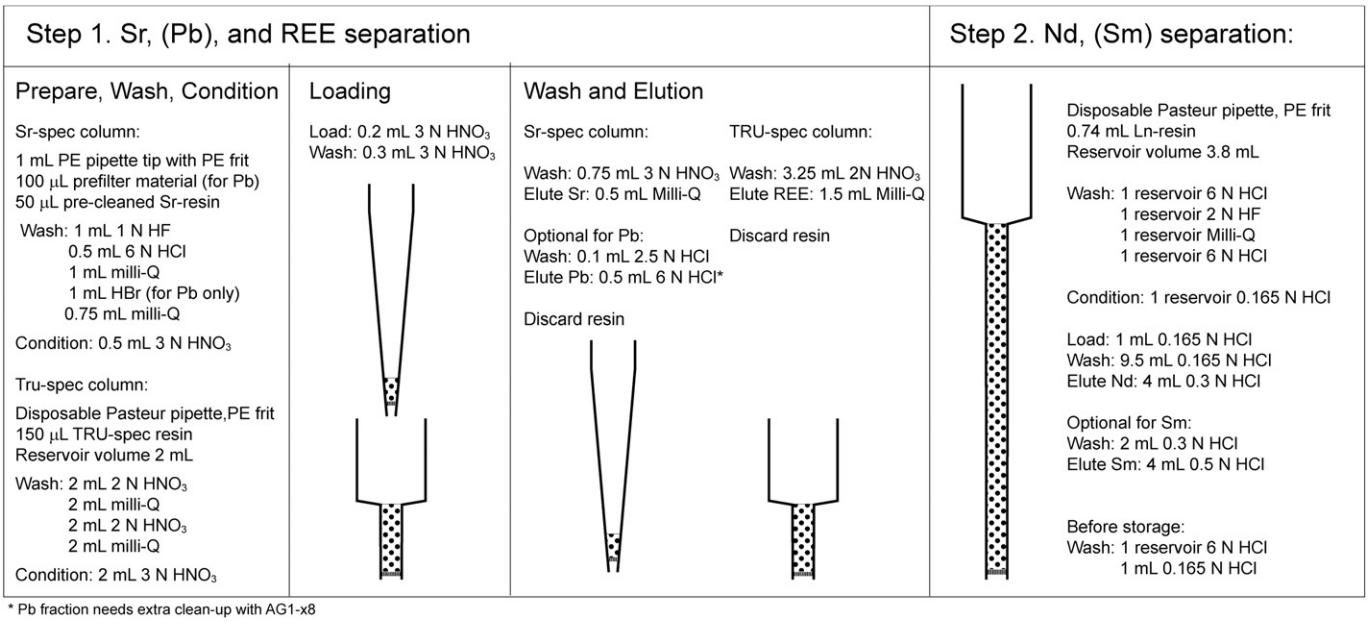

Fig. 5. Schematic overview of the miniaturised chemical separation method for Sr and Nd in melt inclusions.

Table 2
Sr and Nd isotope data for melt inclusions and host lavas.

Volcanic centre	Sample	$^{87}Sr/^{86}Sr$	$2SE * 10^{-6}$	$^{143}Nd/^{144}Nd$	$2SE * 10^{-5}$
Melt inclusions					
Torre Alfina	TA-15	0.714045	30	0.51199	6
	TA-66	0.715429	21	0.51210	7
Vulsini	Vul-28	0.709744	8	0.51216	7
	Vul-21	0.709777	8	0.51190	5
Sabatini	Sab-224	0.710156	11	0.51197	7
	Sab-85	0.709560	10	0.51214	4
	Sab85-re-run 10^{11} Ω amplifiers			0.51207	4
Latera	Lat-222	0.709847	11	0.51211	7
	Lat-220	0.709482	17	0.51209	7
	Lat-256	0.709855	27	0.51212	5
	Lat-256 re-run 10^{11} Ω amplifiers			0.51215	6
	Lat-157	0.709841	28	0.51213	5
Roccamonfina	Rocc7-8	0.709838	8	0.51175	5
	Rocc7-265/9	0.709800	10	0.51214	5
	Rocc5-40	0.709435	13	0.51209	6
	Rocc6-107	0.706500	10	0.51235	6
	Rocc6-104	0.706663	32	0.51223	11
Vesuvius	Ves2B-187	0.707462	15	0.51234	8
	Ves2B-176/9	0.707315	7	0.51237	6
	Ves2L-152	0.707661	10	0.51227	7
Vulture	Melf7-57	0.705084	8	0.51262	6
	Melf7-82	0.705337	9	0.51265	5
	Melf7-244	0.705857	9	0.51268	8
Host lavas					
Torre Alfina	Torre Alfina	0.716369	9	0.512055	3
Vulsini	Vulsini12	0.710073	9	0.512140	4
Sabatini	Sabatini6	0.710058	9	0.512084	7
Latera	Latera20	0.709947	9	0.512156	4
	Latera21	0.709972	8	0.512166	6
Roccamonfina	Rocc5	0.708312	8	0.512233	4
	Rocc6	0.706500	8	0.512372	4
	Rocc7	0.709874	11	0.512085	4
Vesuvius	Ves2b	0.707371	10	0.512426	5
	Ves2L	0.707646	8	0.512423	11
Vulture	Vul7	0.705248	10	0.512681	5

(GeoReM preferred value). BHVO-2 gave a $^{143}Nd/^{144}Nd = 0.512890 \pm 113$ and $^{87}Sr/^{86}Sr = 0.703500 \pm 23$, 2SD n = 4 also in agreement with its reference values 0.512980 ± 12 and 0.703469 ± 17. It follows from the rock standard data that the external reproducibility (2SD) is on average a factor of 1.4 larger compared to the propagated internal error (2SE).

3.4. Validation by repeat analyses on 10^{11} Ω amplifiers

Two melt inclusions (Sab-85 and Lat-256) had sufficient Nd to allow a second analysis of the same filament using default 10^{11} Ω amplifiers. First, the samples were run for 260–300 cycles using 10^{13} Ω amplifiers and subsequently they were run to exhaustion using 10^{11} Ω amplifiers. The 2SE error on the first analysis using the 10^{13} Ω amplifiers was always better than 100 ppm before it was stopped for the repeat analysis. The data for these repeat analyses (Table 2) demonstrate excellent reproducibility when using either set of amplifiers, reconfirming the high quality of data collected with the prototype 10^{13} Ω amplifiers. The 2RSD for Sab-85 is 177 ppm and for Lat-256 it is 66 ppm, n = 2. Note that for Sab85 the repeat analysis by 10^{11} Ω amplifiers yielded more precise data because the sample could be run at higher intensities and for larger amounts of cycles. The propagated 2SE for Sab85 using 10^{11} Ω amplifiers is 78 ppm whereas for the 10^{13} Ω amplifier analysis it is 81 ppm.

4. Results

Melt inclusion and host rock Sr and Nd isotope data are presented in Table 2 and displayed in Fig. 7 together with literature data for each locality. $^{87}Sr/^{86}Sr$ ratios in the melt inclusions range from 0.705084 ± 8 to 0.715429 ± 21 and $^{143}Nd/^{144}Nd$ ratios range from 0.51175 ± 5 to 0.51268 ± 8. Host lavas $^{87}Sr/^{86}Sr$ range from 0.705248 ± 10 to 0.716369 ± 9, and $^{143}Nd/^{144}Nd$ from 0.512055 ± 3 to 0.512681 ± 5. These new bulk-rock data are in agreement with the extensive data sets for K-rich lavas from the Italian peninsula available in the literature (Fig. 7).

Four melt inclusions have indistinguishable $^{87}Sr/^{86}Sr$ and $^{143}Nd/^{144}Nd$ compositions from their host lava; 2 inclusions from Vesuvius and 2 inclusions from Vulture (Fig. 7). All other isotopic compositions of melt inclusions differ from the bulk host sample, even though most are within the range defined by bulk lavas for the specific volcanic centre. In five cases the isotope compositions of the inclusions are distinct from both host lava compositions and literature data for that locality. For example, the $^{87}Sr/^{86}Sr$ determined for the melt inclusions from Torre Alfina and Latera volcanoes plots at lower $^{87}Sr/^{86}Sr$ compared to the fields defined by lavas for each of these localities (Fig. 7), while the Nd isotope compositions of three melt inclusions from Vulsini, Sabatini, and Roccamonfina plot below the fields defined by lava compositions for the host volcano (Fig. 7).

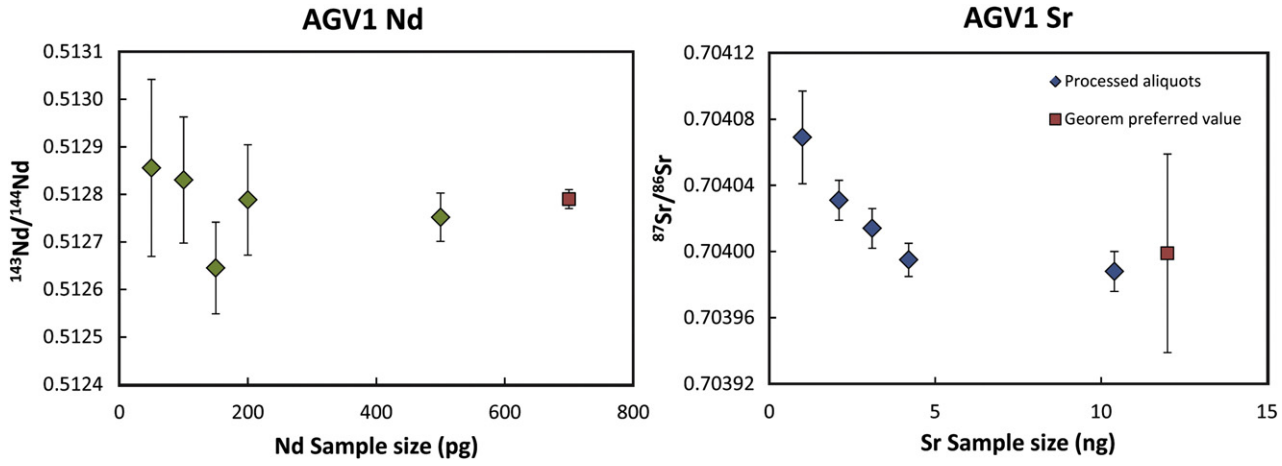

Fig. 6. To validate the techniques $^{143}Nd/^{144}Nd$ (left) and $^{87}Sr/^{86}Sr$ (right) were determined on small aliquots of AGV-1. Aliquots were processed to contain 50, 100, 150, 200 and 500 pg of Nd corresponding to ~1, 2, 3, 4 and 10 ng Sr.

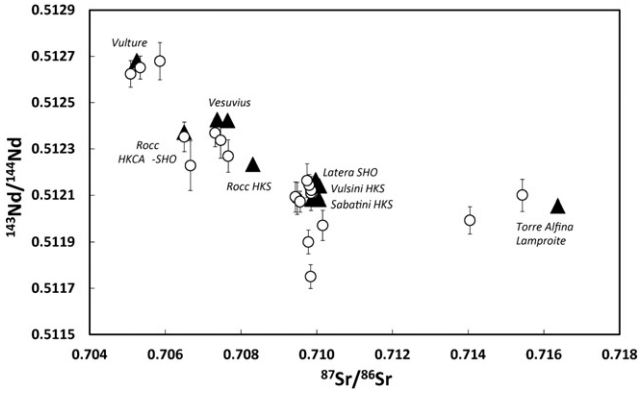

Fig. 7. Overview of the $^{87}Sr/^{86}Sr$ versus $^{143}Nd/^{144}Nd$ data for the melt inclusions (open circles) compared to host lavas (filled triangles) for all sample localities.

5. Discussion

5.1. Significance of observed variability

Multiple analyses of small aliquots of international reference materials AGV-1 and BHVO-2 demonstrated that samples with 150 pg Nd and 3 ng Sr yield accurate and reproducible data (Section 3.3). These data validate our combined miniaturised chemical separation and the Sr and Nd analysis techniques. The external errors (2SD) for the Nd and Sr analyses suggest that variability larger than 220 ppm for $^{143}Nd/^{144}Nd$ and 33 ppm for $^{87}Sr/^{86}Sr$ can be resolved using our techniques on such small samples. For our melt inclusions we had generally more than 150 pg Nd and 3 ng Sr available (Table 1). Therefore, we consider the reproducibility tests on the international standards as yielding maximum errors for the analysed melt inclusions.

The differences in isotopic composition between host lava and individual melt inclusions are in most cases significantly larger than the external reproducibility of the measurements (Table 2; Fig. 8). Expressed relative to the host lava, the difference in $^{87}Sr/^{86}Sr$ between inclusions and lavas is up to 3‰ for Torre Alfina for example. This difference is a factor of 100 larger than the external reproducibility of 33 ppm. For Vulsini, Latera, and Roccamonfina the $^{87}Sr/^{86}Sr$ of inclusions and hosts differs by 463 ppm, 650 ppm and 1.6‰ respectively, factors of 14, 20 and 48 larger than the 2RSD on the $^{87}Sr/^{86}Sr$ ratio. In 3 cases $^{143}Nd/^{144}Nd$ ratio differs significantly between melt inclusions and host lavas. For Roccamonfina, for example the difference is 653 ppm; a factor of 3 larger than the external reproducibility of 220 ppm. This quantitative comparison with the obtained external analytical error confirms the significance of the measured isotopic variability. Excellent reproducibility for repeat analyses of melt inclusions Sab85 and Lat256 using 10^{13} and 10^{11} Ω amplifiers (see Section 3.4) reinforces the validity of our techniques.

No blank corrections could be performed to the $^{87}Sr/^{86}Sr$ data since the exact amounts of Sr within the processed inclusions were unknown. Five of the selected inclusions were estimated to contain less than 3 ng Sr (Table 1) suggesting a possible contribution of a chemistry blank. The sample with the lowest estimated Sr content (Lat-157) yielded a Sr isotope composition indistinguishable from that of two other Latera melt inclusions ($^{87}Sr/^{86}Sr = 0.709841 \pm 28$), lower than that of the host lava ($^{87}Sr/^{86}Sr = 0.709947 \pm 9$). The expected effect of a contribution of a procedural blank would be to shift the measured value to higher $^{87}Sr/^{86}Sr$ as the isotope composition of our procedural blank is $^{87}Sr/^{86}Sr = 0.71112 \pm 5$ (see Section 3.3). If we assume that the sample was affected by a procedural blank of 10 pg the $^{87}Sr/^{86}Sr$ would have been ~0.7094, similar to that of inclusion Lat-220 and still significantly lower than the host lava value.

5.2. Comparison with previous melt inclusion isotope analyses and method limitations

Sr and Pb isotope compositions of individual melt inclusions have previously been determined by in situ techniques (Saal et al., 1998, 2005; Jochum et al., 2004; Jackson and Hart, 2006; Nikogosian et al., 2007; Maclennan, 2008; Paul et al., 2011; Sobolev et al., 2011; Rose-Koga et al., 2012). Far more Pb isotope data have been produced than Sr isotope data, presumably because the latter are compromised by isobaric interfering isotopes such as ^{87}Rb and ^{86}Kr. The Rb interference limits the precision, due to uncertainty associated with the Rb correction. A corrected $^{87}Sr/^{86}Sr$ ratio exhibits an error magnification that is directly proportional to the Rb/Sr ratio of the sample (Jackson and Hart, 2006). These authors reported an upper limit for the external precision on $^{87}Sr/^{86}Sr$ of 335 ppm (2SD) based on analysis of 7 inclusions from Samoan basalt with low Rb (Rb/Sr = 0.053), using a 213 nm NewWave laser ablation system coupled to a Thermo-Finnigan Neptune MC-ICPMS. Sobolev et al. (2011) analysed combined Sr and Pb isotopes at precisions of 0.04–0.2% for $^{87}Sr/^{86}Sr$ and 0.1% for $^{208}Pb/^{206}Pb$ and $^{207}Pb/^{206}Pb$, using a New Wave 193 nm laser ablation system coupled to a Thermo Element2 ICP-MS. Compared to these previous results our technique to determine $^{87}Sr/^{86}Sr$ produces significantly more precise data (2RSD of 33 ppm). Although this better precision comes with the relatively time-consuming step required for chemical separation, our procedure allows us to analyse Rb-rich samples. In addition, it allows precise determinations of coupled Sr–Nd isotope compositions for melt inclusion studies.

The limitation of the presented technique currently lies within the Sr procedural blank which requires Sr sample sizes to be larger than 2 ng. Despite thorough cleaning of lab ware and minimisation of the volumes used in the elemental separation procedures, our Sr blank levels vary between 3 and 20 pg. The lower limit of Sr required for an analysis currently determines the minimum size of an inclusion at a certain concentration level. For inclusions with high Sr concentrations (>1000 ppm), as often the case in subduction related settings, the analyses of single inclusions with a diameter >100 μm are viable (Fig. 2). When inclusions have lower Sr concentrations, for instance in a NMORB settings (<100 ppm Sr), an accurate Sr analysis can only be performed on a single inclusion with a relatively large size (>230 μm diameter). Reduction of Sr blank levels to sub ng levels would be required if the size is smaller. Because our Nd analyses on single melt inclusions are not compromised by the procedural blank, an analysis of a single inclusion with NMORB-like composition (~10 ppm Nd) is viable for inclusions with a minimum diameter of 120 μm (Fig. 2). For such a small Nd analysis, however, (30 pg Nd) the measurement error (2RSE ~ 300 ppm) will likely become an issue in view of the usually limited isotope variability in NMORB settings. Problems with the Sr blank and the analytical error on Nd could be avoided by selecting melt inclusions of a similar type and pooling them for the measurements. Obviously, this strategy requires careful petrological characterisation of host olivine and/or the inclusions themselves. Grouping of melt inclusions based on minor element compositions (e.g., CaO and NiO) of olivine is relatively straightforward (e.g. Elburg et al., 2006; Kamenetsky et al., 2006). Detailed major and trace element characterisation of the inclusions themselves (Nikogosian and van Bergen, 2010) would be a more reliable and preferred approach, but is much more time consuming as it requires homogenisation, polishing and analysis by microbeam techniques.

5.3. Isotopic contrasts between melt inclusions and host lavas

Based on the combined Sr and Nd isotope data for melt inclusions and host lavas we distinguish three different scenarios: 1) the melt inclusions and their host lavas have identical Sr and Nd isotope compositions; 2) the melt inclusions have either different Sr or different Nd isotope compositions; and 3) neither Nd nor Sr isotope ratios are

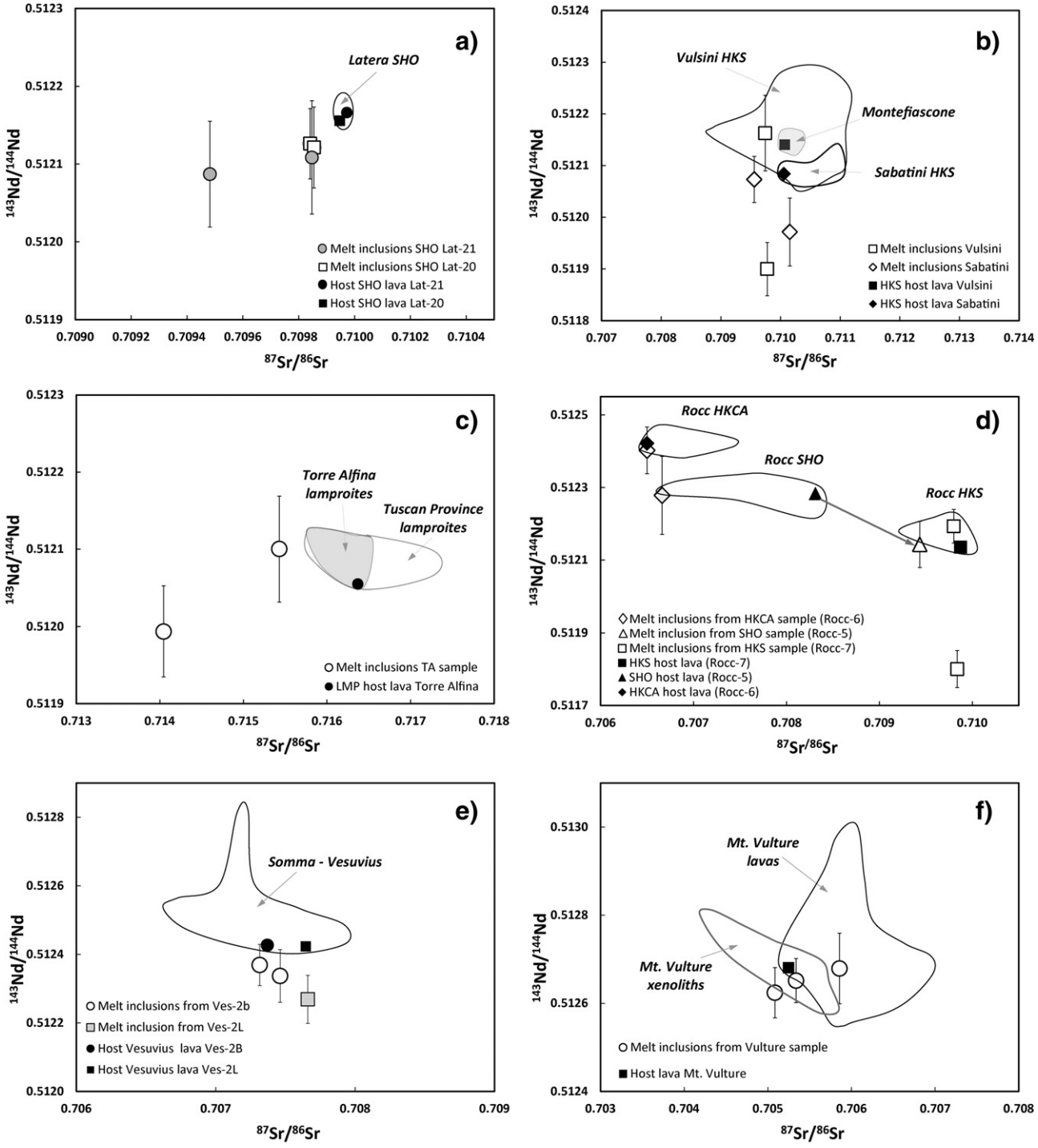

Fig. 8. $^{87}Sr/^{86}Sr$ versus $^{143}Nd/^{144}Nd$ data per locality (a. Latera; b. Vulsini–Sabatini; c. Torre Alfina; d. Roccamonfina; e. Somma–Vesuvius; f. Vulture) for a more detailed comparison of melt inclusion data with the host lava and literature lava compositions. Data used to draw the literature fields are from Lustrino et al. (2011) and references therein; D'Orazio et al. (2007), De Astis et al. (2006), and Downes et al. (2002). The arrow in (d) indicates the link between the melt inclusion and its host lava. Note that the inclusion rocc-5 plots in the field of HKS lavas suggesting that a HKS type olivine was entrained by shoshonite magma.

identical for melt inclusions and host rocks. The cases of different isotope compositions reflect dissimilar evolution histories for the primitive melt that was trapped as inclusion in an olivine phenocryst and melt that is represented by the groundmass of the host lava. Potential processes responsible for isotopic inhomogeneity in a single lava sample are:

- Mixing/mingling of magmas with different isotope signatures. This process creates textural and compositional disequilibrium between lavas and xeno/phenocrysts, and is a widespread phenomenon in the potassium-rich magmatic systems of mainland Italy (Civetta et al., 1981; Barton et al., 1982; Giannetti and Luhr, 1983; Giannetti and Ellam, 1994; Nikogosian and van Bergen, 2010).
- Assimilation of crustal rocks with contrasting isotopic composition. Interaction of magmas with crustal rocks, particularly Mesozoic limestones, is relatively common in Italy and has been inferred for several of the studied volcanic centres (Marziano et al., 2008; Peccerillo et al., 2010; Conticelli et al., 2013).

- Melt extraction from a heterogeneous mantle source. Melting of a heterogeneous mantle results in formation of melts with variable isotopic compositions. Bulk lavas derived from a heterogeneous mantle represent accumulated melts that are mixed and homogenised before eruption. If melt inclusions are trapped deep within the magmatic plumbing system they have the potential to record much more heterogeneity compared to the accumulated bulk lavas (Saal et al., 1998, 2005; Jackson and Hart, 2006; Sobolev et al., 2011). The large variability in Sr–Nd–Pb isotope compositions found in Italian magmatism has been explained by melting of a veined metasomatised sub-continental lithospheric mantle that resulted from subduction and input of variable amounts and types of sediments (Foley, 1992; Conticelli et al., 2002, 2009; Boari et al., 2009). Primitive melt inclusions from Italy may thus record larger isotope variability than the host lavas and provide better constraints on the mantle components.

Below we will illustrate how isotopic differences between melt inclusion and host lava (Fig. 8) can place constraints on the evolution of a magmatic system that would not be possible with whole-rock results alone. The potential processes listed above and existing information for each of the localities will be used as guidelines.

5.3.1. Latera

Four melt inclusions from two samples of a shoshonitic lava flow from Latera volcano (Fig. 8a) yield Nd isotope compositions identical to those of the host lavas when considering the analytical uncertainties. In contrast, their Sr isotope ratios are significantly less radiogenic than the bulk rock lavas. For example, the two inclusions Lat-220 and Lat-222 in host Lat-21 have dissimilar Sr isotope compositions and differ from the host by 0.65‰ and 0.15‰ respectively, indicating significant internal heterogeneity within this sample. These observations suggest involvement of isotopically heterogeneous melts in the plumbing system during early olivine growth. The higher Sr isotope ratios of samples from the lava reflect the addition of a more radiogenic component possibly via crustal assimilation or magma mixing after the inclusions were trapped. The small range in Sr isotope compositions for bulk Latera lavas suggests that the magma became homogenised prior to eruption. These explanations for the isotopic relationships are consistent with earlier petrological evidence for contributions of multiple mantle derived melts to the late-stage effusive and strombolian products of the Latera complex, admixture of a distinct lamproitic component to the shoshonitic magma and for the role of crustal assimilation and the presence of potential assimilants with high $^{87}Sr/^{86}Sr$ in the subsurface (Ferrara et al., 1986; Varekamp and Kalamarides, 1989; Conticelli et al., 1991).

5.3.2. Vulsini and Sabatini

The four melt inclusions in two HKS lava samples from Vulsini and Sabatini volcanic complexes have $^{87}Sr/^{86}Sr$ ratios that overlap with the data range for bulk lavas reported in the literature (Fig. 8b). Minor but significant differences exist, however, between the inclusions and their hosts, with the inclusions tending to be less radiogenic (up to 0.46‰ difference). The inclusions also show considerable variation in $^{143}Nd/^{144}Nd$, ranging from similar to the host rock towards significantly lower values than the HKS lavas from Vulsini and Sabatini (0.47‰ and 0.22‰ difference, see Fig. 8b). The K-rich magmas in these regions are known to have locally interacted with Mesozoic limestone that have lower $^{143}Nd/^{144}Nd$ ratios than the volcanics (Peccerillo et al., 2010). Such a late-stage open-system process, however, is an unlikely explanation for the observed low Nd isotopes in the melt inclusions, as the high REE concentrations in mafic HKS magmas would imply large amounts of limestone assimilation, unrealistic in view of the primitive nature and early entrapment of the inclusions. In addition, assimilation of the local limestone is expected to lower the $^{87}Sr/^{86}Sr$ ratios of magmas (Peccerillo et al., 2010) given the highly radiogenic nature of the ultrapotassic primary melts and would therefore result in a melt inclusion–host lava relationship opposite to that observed. Instead, our results are more in accordance with a temporary co-existence of different primitive melts shortly after segregation from an isotopically heterogeneous mantle. This mantle presumably contains an unradiogenic Nd isotope component that has so far remained unnoticed in bulk-rock data. These inferences are consistent with the widespread evidence for veined or otherwise inhomogeneous mantle sources of the HKS magmas in these regions, attributable to heterogeneous subduction-related metasomatic enrichments in sedimentary components (Conticelli and Peccerillo, 1992; Kamenetsky et al., 1995; Conticelli et al., 2002; Peccerillo, 2005).

5.3.3. Torre Alfina

The two melt inclusions from the Torre Alfina lamproite have $^{143}Nd/^{144}Nd$ identical to the host lava and overlap with the data for the bulk lavas reported in the literature (Fig. 8c). The $^{87}Sr/^{86}Sr$ ratios in the melt inclusions, however, differ from each other and are significantly less radiogenic than the host lava (1‰ and 3‰). Assimilation of a component with radiogenic Sr is a plausible explanation since the Torre Alfina lavas show an increase in $^{87}Sr/^{86}Sr$ with increasing SiO_2 and contain gneiss xenoliths from the metasedimentary basement (Ferrara et al., 1986; Conticelli, 1998). Whether interaction with basement rocks is also responsible for the isotopic difference between the melt inclusions is questionable in view of the primitive nature of both inclusions and the substantial amount of assimilation that would be required to create the observed shift, given the relatively low Sr content of the potential assimilant (~200 ppm, Ferrara et al., 1986). Instead, the melt inclusions appear to have inherited their Sr isotope signatures from an isotopically heterogeneous mantle source.

5.3.4. Roccamonfina

The studied melt inclusions from Roccamonfina volcano are from samples of three rock series (HKCA, SHO and HKS) with different Sr–Nd isotope compositions (Fig. 8d). Of the two analysed melt inclusions from the HKCA lava, one is identical to the host, whereas the other has higher Sr and a lower Nd isotope ratios, so that it plots at the margin of the field defined by SHO lavas of Roccamonfina. This second melt inclusion was specifically selected because of its shoshonitic major and trace element composition that had been taken as evidence for mixing/mingling processes within the plumbing system of this volcano (Nikogosian and van Bergen, 2010). The $^{87}Sr/^{86}Sr$ and $^{143}Nd/^{144}Nd$ ratios determined for this inclusion support this interpretation.

Likewise, a melt inclusion from a SHO lava was selected for analysis because of its major and trace element similarities with HKS lavas. This inclusion has significantly lower $^{87}Sr/^{86}Sr$ (1.6‰) and $^{143}Nd/^{144}Nd$ (0.27‰) than its host, and indeed overlaps the field of Roccamonfina HKS lavas (Fig. 8d). Both examples thus demonstrate the presence of forsteritic olivine populations from other rock series in HKCA and SHO lavas, and confirm mineralogical and chemical evidence for mixing/mingling of magmas with different serial affinities (Giannetti and Luhr, 1983).

The two melt inclusions from the HKS lava have Sr isotope compositions identical to that of the host lava but show significant Nd isotope variation. One is close to the host lava whereas the other has 0.65‰ lower $^{143}Nd/^{144}Nd$. The inclusions were selected for analysis because of their strong contrast in major and trace element compositions (Fig. 3), thought to result from selective melt extraction from a metasomatised mantle. According to Nikogosian and Van Bergen (2010), the primitive HKS magmas of Roccamonfina represent collections of mixed primary melts. Strong chemical heterogeneity of Mg-rich melt inclusions suggests that melts represent progressive stages of melt extraction from a chemically and mineralogically heterogeneous mantle that were trapped in olivine phenocrysts before a sizeable volume of relatively homogeneous magma could form and

rise to the surface. Since the inclusion with the lowest $^{143}Nd/^{144}Nd$ belongs to a subgroup of melt inclusions with carbonatitic affinity (e.g. low K_2O and Rb/Sr; high CaO, Ba/Cs and La/Yb) and the other inclusions to a more strongly potassic subgroup (Nikogosian and Van Bergen, 2010), the observed contrast in Nd suggests that the mantle source of HKS magma is isotopically heterogeneous. We speculate that the K-rich silicic and carbonatite-like components of metasomatic agents created a veined source domain below Roccamonfina that is reflected by isotopic inhomogeneity of the melt inclusions (Conticelli et al., 2009; Nikogosian and Van Bergen, 2010). A separate hybrid source has also been inferred for the HKCA and SHO magmas, based on the Sr isotope variability of mafic lavas from these series (Giannetti and Ellam, 1994). These combined compositional relationships testify that local heterogeneities in mantle source can be traced with isotopic analysis of individual melt inclusions.

5.3.5. Vesuvius

Three melt inclusions from two HKS lavas of Vesuvius show similar $^{87}Sr/^{86}Sr$ ratios to their hosts and overlap with compositions reported for other lavas (Fig. 8e). Nd isotope compositions of two inclusions are within error of the host lava but one inclusion has a significantly lower $^{143}Nd/^{144}Nd$ value (0.3‰) and other Vesuvius lavas. Earlier evidence for isotopic variability in Vesuvius products comes from inhomogeneity of bulk samples from individual lavas and contrasts between phenocrysts and bulk host samples (Caprarelli et al., 1993; Ayuso et al., 1998; Piochi et al., 2006 and references therein). It is widely accepted that the potassic parental magmas of Somma–Vesuvius originate from a metasomatically enriched mantle source. Changes in the Sr–Nd isotope signatures in the history of the complex can be attributed to the combined effects of heterogeneity in the mantle source, interaction or assimilation of carbonates and other shallow crustal rocks, and entrapment of crystal mush generated during previous magma storage in the crust (Ayuso et al., 1998; Piochi et al., 2006).

5.3.6. Vulture

Three melt inclusions from Vulture volcano have $^{143}Nd/^{144}Nd$ ratios that are indistinguishable from the Vul 7 host lava. Their Sr isotope compositions, however, show significant variability (1‰; Fig. 8f). The Sr isotope composition of one inclusion plots outside the field defined by melilitic, foiditic, carbonatitic and more evolved products of Vulture (De Astis et al., 2006; D'Orazio et al., 2007), but coincides with data reported for local mantle xenoliths (Downes et al., 2002). Within this context, the melt-inclusion data are consistent with the presence of heterogeneous near-primary melts within the plumbing system of the complex.

6. Conclusions

We determined Sr and Nd isotope compositions by TIMS in individual olivine-hosted melt inclusions from a variety of mafic potassium-rich lavas from Neogene–Quaternary volcanic centres in mainland Italy with the aim of testing a novel TIMS technique for the analysis of small geological samples. Sr isotopes were measured using default 10^{11} Ω amplifiers, whereas Nd isotope compositions were determined using new 10^{13} Ω amplifiers that were designed to measure small ion beams at relatively high precision. A miniaturised Sr and Nd chemical separation procedure was used to keep procedural blanks to a minimum. Small aliquots of international rock standards were used to check for accuracy and reproducibility. Samples as small as 2 ng Sr and 30 pg Nd were analysed successfully. Compared to previous techniques that analysed Sr isotopes in melt inclusions in situ, our approach is not limited by the amount of Rb present in a sample, which greatly expands the compositional range of samples that can be analysed.

Our data cover a large range in Sr and Nd isotope compositions as expected for the Italian peninsula illustrating the applicability of the technique. The data, however, also expose inhomogeneity in $^{87}Sr/^{86}Sr$ and/or $^{143}Nd/^{144}Nd$ ratios when comparing the isotopic compositions of primitive melt inclusions and studied bulk Italian lavas. The detected differences between inclusions and host lavas point to different evolution histories of melts trapped in early crystallised phases and those that are represented by the groundmass. In line with magmatic processes known to have affected Italian potassic volcanics, such features can be attributed to mixing and mingling of isotopically distinct magma batches, assimilation of crustal material with different isotope compositions or early (incomplete) mixing of primitive melts derived from an isotopically heterogeneous mantle source. The presented examples demonstrate the potential of our methodology to analyse individual melt inclusions for detailed studies of magma evolution processes. Further more detailed work is required to fully quantify the processes responsible for the isotopic variability recorded in magmatism from the Italian peninsula. Currently the applicability of the technique is not limited by the Nd content as would be expected owing to generally lower Nd concentrations compared to Sr concentrations in lavas, but rather by the Sr concentration and size of the melt inclusions because of the inability to correct for the procedural Sr blanks (3–20 pg). For an accurate Sr analysis with the current technique we need 2 ng Sr, implying that an inclusion with 100 ppm Sr (NMORB) should have a diameter of 225 μm. Blank levels should be further reduced for melt inclusions with lower concentrations or smaller volumes.

Acknowledgements

We thank two anonymous reviewers for their helpful comments and suggestions. Financial support for this project was provided by the Netherlands Organisation for Scientific Research (NWO, grant number 834.10.001) and the Netherlands Research Centre for Integrated Solid Earth Science (ISES) through grant 6.2.12.

References

Avanzinelli, R., Lustrino, M., Mattei, M., Melluso, L., Conticelli, S., 2009. Potassic and ultrapotassic magmatism in the circum-Tyrrhenian region: significance of carbonated pelitic vs. pelitic sediment recycling at destructive plate margins. Lithos 113 (1–2), 213–227.

Ayuso, R.A., De Vivo, B., Rolandi, G., Seal, R.R., Paone, A., 1998. Geochemical and isotopic (Nd–Pb–Sr–O) variations bearing on the genesis of volcanic rocks from Vesuvius, Italy. J. Volcanol. Geotherm. Res. 82 (1–4), 53–78.

Barton, M., Varekamp, J.C., Vanbergen, M.J., 1982. Complex zoning of clinopyroxene in the lavas of Vulsini, Latium, Italy — evidence for magma mixing. J. Volcanol. Geotherm. Res. 14 (3–4), 361–388.

Boari, E., Tommasini, S., Laurenzi, M.A., Conticelli, S., 2009. Transition from ultrapotassic kamafugitic to sub-alkaline magmas: Sr, Nd, and Pb isotope, trace element and Ar-40–Ar-39 age data from the Middle Latin Valley Volcanic Field, Roman Magmatic Province, Central Italy. J. Petrol. 50 (7), 1327–1357.

Caprarelli, G., Togashi, S., Devivo, B., 1993. Preliminary Sr and Nd isotopic data for recent lavas from Vesuvius volcano. J. Volcanol. Geotherm. Res. 58 (1–4), 377–381.

Civetta, L., Innocenti, F., Manetti, P., Peccerillo, A., Poli, G., 1981. Geochemical characteristics of potassic volcanics from Mts Ernici (Southern Latium, Italy). Contrib. Mineral. Petrol. 78 (1), 37–47.

Civetta, L., Gallo, G., Orsi, G., 1991. Sr-isotope and Nd-isotope and trace-element constraints on the chemical evolution of the magmatic system of Ischia (Italy) in the last 55 ka. J. Volcanol. Geotherm. Res. 46 (3–4), 213–230.

Conticelli, S., 1998. The effect of crustal contamination on ultrapotassic magmas with lamproitic affinity: mineralogical, geochemical and isotope data from the Torre Alfina lavas and xenoliths, Central Italy. Chem. Geol. 149 (1–2), 51–81.

Conticelli, S., Peccerillo, A., 1992. Petrology and geochemistry of potassic and ultrapotassic volcanism in central Italy — petrogenesis and inferences on the evolution of mantle sources. Lithos 28 (3–6), 221–240.

Conticelli, S., Francalanci, L., Santo, A.P., 1991. Petrology of final-stage Latera lavas (Vulsini Mts) — mineralogical, geochemical, and Sr-isotopic data and their bearing on the genesis of some potassic magmas in central Italy. J. Volcanol. Geotherm. Res. 46 (3–4), 187–212.

Conticelli, S., D'Antonio, M., Pinarelli, L., Civetta, L., 2002. Source contamination and mantle heterogeneity in the genesis of Italian potassic and ultrapotassic volcanic rocks: Sr–Nd–Pb isotope data from Roman Province and Southern Tuscany. Mineral. Petrol. 74 (2–4), 189–222.

Conticelli, S., et al., 2009. Shoshonite and sub-alkaline magmas from an ultrapotassic volcano: Sr–Nd–Pb isotope data on the Roccamonfina volcanic rocks, Roman Magmatic Province, Southern Italy. Contrib. Mineral. Petrol. 157 (1), 41–63.

Conticelli, S., Avanzinelli, R., Marchionni, S., Tommasini, S., Melluso, L., 2011. Sr–Nd–Pb isotopes from the Radicofani Volcano, Central Italy: constraints on heterogeneities

in a veined mantle responsible for the shift from ultrapotassic shoshonite to basaltic andesite magmas in a post-collisional setting. Mineral. Petrol. 103 (1–4), 123–148.
Conticelli, S., Avanzinelli, R., Poli, G., Braschi, E., Giordano, G., 2013. Shift from lamproite-like to leucititic rocks: Sr–Nd–Pb isotope data from the Monte Cimino volcanic complex vs. the Vico stratovolcano, Central Italy. Chem. Geol. 353, 246–266.
De Astis, G., Kempton, P.D., Peccerillo, A., Wu, T.W., 2006. Trace element and isotopic variations from Mt. Vulture to Campanian volcanoes: constraints for slab detachment and mantle inflow beneath southern Italy. Contrib. Mineral. Petrol. 151 (3), 331–351.
De Hoog, J.C.M., Gall, L., Cornell, D.H., 2010. Trace-element geochemistry of mantle olivine and application to mantle petrogenesis and geothermobarometry. Chem. Geol. 270 (1–4), 196–215.
D'Orazio, M., Innocenti, F., Tonarini, S., Doglioni, C., 2007. Carbonatites in a subduction system: the Pleistocene alvikites from Mt. Vulture (Southern Italy). Lithos 98 (1–4), 313–334.
Downes, H., et al., 2002. Geochemistry and Sr–Nd isotopic compositions of mantle xenoliths from the Monte Vulture carbonatite–melilitite volcano, central southern Italy. Contrib. Mineral. Petrol. 144 (1), 78–92.
Elburg, M., Kamenetsky, V.S., Nikogosian, I., Foden, J., Sobolev, A.V., 2006. Coexisting high- and low-calcium melts identified by mineral and melt inclusion studies of a subduction-influenced syncollisional magma from South Sulawesi, Indonesia. J. Petrol. 47 (12), 2433–2462.
Ferrara, G., Preitemartinez, M., Taylor, H.P., Tonarini, S., Turi, B., 1986. Evidence for crustal assimilation, mixing of magmas, and a Sr-87-rich upper mantle — an oxygen and strontium isotope study of the M-Vulsini volcanic area, Central Italy. Contrib. Mineral. Petrol. 92 (3), 269–280.
Foley, S., 1992. Vein-plus-wall-rock melting mechanisms in the lithosphere and the origin of potassic alkaline magmas. Lithos 28 (3–6), 435–453.
Font, L., et al., 2012. Strontium and lead isotope ratios in human hair: investigating a potential tool for determining recent human geographical movements. J. Anal. At. Spectrom. 27 (5), 719–732.
Giannetti, B., Ellam, R., 1994. The primitive lavas of Roccamonfina Volcano, Roman Region, Italy — new constraints on melting processes and source mineralogy. Contrib. Mineral. Petrol. 116 (1–2), 21–31.
Giannetti, B., Luhr, J.F., 1983. The white trachytic tuff of Roccamonfina Volcano (Roman Region, Italy). Contrib. Mineral. Petrol. 84 (2–3), 235–252.
Jackson, M.G., Hart, S.R., 2006. Strontium isotopes in melt inclusions from Samoan basalts: implications for heterogeneity in the Samoan plume. Earth Planet. Sci. Lett. 245 (1–2), 260–277.
Jakopič, R., et al., 2009. Isotope ratio measurements of pg-size plutonium samples using TIMS in combination with "multiple ion counting" and filament carburization. Int. J. Mass Spectrom. 279 (2–3), 87–92.
Jochum, K.P., Stoll, B., Herwig, K., Hofmann, A.W., 2004. Pb isotopes and trace elements in melt inclusions from Hawaiian basalts using LA-ICPMS and SR-XRF. Geochim. Cosmochim. Acta 68 (11), A564-A564.
Jochum, K.P., et al., 2011. GSD-1G and MPI-DING reference glasses for in situ and bulk isotopic determination. Geostand. Geoanal. Res. 35 (2), 193–226.
Kamenetsky, V., Metrich, N., Cioni, R., 1995. Potassic primary melts of Vulsini (Roman Province) — evidence from mineralogy and melt inclusions. Contrib. Mineral. Petrol. 120 (2), 186–196.
Kamenetsky, V.S., Elburg, M., Arculus, R., Thomas, R., 2006. Magmatic origin of low-Ca olivine in subduction-related magmas: co-existence of contrasting magmas. Chem. Geol. 233 (3–4), 346–357.
Koornneef, J.M., et al., 2009. Nature and timing of multiple metasomatic events in the subcratonic lithosphere beneath Labait, Tanzania. Lithos 112, 896–912.
Koornneef, J.M., Bouman, C., Schwieters, J.B., Davies, G., 2013. Use of 10^{12} Ohm Current Amplifiers in Sr and Nd Isotope Analyses by TIMS for Application to Sub-nanogram Samples. J. Anal. At. Spectrom. 28, 749–754.
Koornneef, J.M., Bouman, C., Schwieters, J.B., Davies, G.R., 2014. Measurement of small ion beams by thermal ionisation mass spectrometry using new 10^{13} Ohm resistors. Anal. Chim. Acta. 819, 49–55.
Liu, J., Pearson, D.G., 2014. Rapid, precise and accurate Os isotope ratio measurements of nanogram to sub-nanogram amounts using multiple Faraday collectors and amplifiers equipped with 10^{12} Ω resistors by N-TIMS. Chem. Geol. 363, 301–311.
Lustrino, M., Duggen, S., Rosenberg, C.L., 2011. The Central-Western Mediterranean: anomalous igneous activity in an anomalous collisional tectonic setting. Earth Sci. Rev. 104 (1–3), 1–40.
Maclennan, J., 2008. Lead isotope variability in olivine-hosted melt inclusions from Iceland. Geochim. Cosmochim. Acta 72 (16), 4159–4176.
Marziano, G.I., Gaillard, F., Pichavant, M., 2008. Limestone assimilation by basaltic magmas: an experimental re-assessment and application to Italian volcanoes. Contrib. Mineral. Petrol. 155 (6), 719–738.
Mikova, J., Denkova, P., 2007. Modified chromatographic separation scheme for Sr and Nd isotope analysis in geological silicate samples. J. Geosci. 52 (3–4), 221–226.
Nikogosian, I.K., van Bergen, M.J., 2009. Unraveling the sources of Italian K-rich volcanism with melt inclusions. Geochim. Cosmochim. Acta 73 (13, Supplement), A943 (Goldschmidt Abstracts 2009).
Nikogosian, I.K., van Bergen, M.J., 2010. Heterogeneous mantle sources of potassium-rich magmas in central-southern Italy: melt inclusion evidence from Roccamonfina and Ernici (Mid Latina Valley). J. Volcanol. Geotherm. Res. 197 (1–4), 279–302.
Nikogosian, I.K., Van Bergen, M.J., De Hoog, J.C., Whitehouse, M.J., Van den Boorn, S.H.J.M., 2007. Extreme Pb-isotope diversity in the sources of K-rich magmas in Italy: evidence from melt inclusions. Geochim. Cosmochim. Acta 71 (15), A719-A719.
Paul, B., et al., 2011. Melt inclusion Pb-isotope analysis by LA-MC-ICPMS: assessment of analytical performance and application to OIB genesis. Chem. Geol. 289 (3–4), 210–223.
Peccerillo, A., 2005. Plio-Quaternary Volcanism in Italy: Petrology, Geochemistry, Geodynamics. Springer-Verlag, Berlin, Germany (365 pp).
Peccerillo, A., Lustrino, M., 2005. Compositional variations of Plio-Quaternary magmatism in the circum-Tyrrhenian area: deep versus shallow mantle processes. Geol. Soc. Am. Spec. Pap. 388, 421–434.
Peccerillo, A., Federico, M., Barbieri, M., Brilli, M., Wu, T.-W., 2010. Interaction between ultrapotassic magmas and carbonate rocks: evidence from geochemical and isotopic (Sr, Nd, O) compositions of granular lithic clasts from the Alban Hills Volcano, Central Italy. Geochim. Cosmochim. Acta 74 (10), 2999–3022.
Pin, C., Zalduegui, J.F.S., 1997. Sequential separation of light rare-earth elements, thorium and uranium by miniaturized extraction chromatography: application to isotopic analyses of silicate rocks. Anal. Chim. Acta. 339 (1–2), 79–89.
Piochi, M., Ayuso, R.A., De Vivo, B., Somma, R., 2006. Crustal contamination and crystal entrapment during polybaric magma evolution at Mt. Somma–Vesuvius volcano Italy: geochemical and Sr isotope evidence. Lithos 86 (3–4), 303–329.
Rose-Koga, E.F., et al., 2012. Mantle source heterogeneity for South Tyrrhenian magmas revealed by Pb isotopes and halogen contents of olivine-hosted melt inclusions. Chem. Geol. 334, 266–279.
Saal, A.E., Hart, S.R., Shimizu, N., Hauri, E.H., Layne, G.D., 1998. Pb isotopic variability in melt inclusions from oceanic island basalts, Polynesia. Science 282 (5393), 1481–1484.
Saal, A.E., et al., 2005. Pb isotopic variability in melt inclusions from the EMI–EMII–HIMU mantle end-members and the role of the oceanic lithosphere. Earth Planet. Sci. Lett. 240 (3–4), 605–620.
Schiavi, F., Kobayashi, K., Nakamura, E., Tiepolo, M., Vannucci, R., 2012. Trace element and Pb–B–Li isotope systematics of olivine-hosted melt inclusions: insights into source metasomatism beneath Stromboli (southern Italy). Contrib. Mineral. Petrol. 163 (6), 1011–1031.
Schwieters, J., H. Lerche, Thermo Electron, (Bremen), US Patent 6,472,659 B1, issued 29/10/2002. Method for measuring ionic currents, and a catching device. Thermo Electron (Bremen).
Sobolev, A.V., Hofmann, A.W., Jochum, K.P., Kuzmin, D.V., Stoll, B., 2011. A young source for the Hawaiian plume. Nature 476 (7361), 434–437.
Tuttas, D., Schwieters, J.B., Quaas, N., Bouman, C., 2007. Improvements in TIMS High Precision Isotope Ratio Measurements for Small Sample Sizes. Thermo Fischer Scientific, Bremen, Germany.
Tuttas, D., Schwieters, J.B., Bouman, C., Deerberg, M., 2008. New Compact Discrete Dynode Multipliers Integrated into the Thermo Scientific TRITON Variable Multicollector Array. Thermo Fischer Scientific, Bremen, Germany.
Vannucci, R., et al., 2006. Recent Stromboli (Italy): insights into magma sources and processes from melt inclusions. Geochim. Cosmochim. Acta 70 (18), A667-A667.
Varekamp, J.C., Kalamarides, R.I., 1989. Hybridization processes in leucite tephrites from Vulsini, Italy, and the evolution of the Italian potassic suite. J. Geophys. Res. Solid Earth Planets 94 (B4), 4603–4618.
Wielandt, D., Bizzarro, M., 2011. A TIMS-based method for the high precision measurements of the three-isotope potassium composition of small samples. J. Anal. At. Spectrom. 26 (2), 366–377.